Table 7 Results of outer boundary-position studies

Case	Grid	Outer boundary	C_l	C_d	$\%C_l$	$\%C_d$
1	493 × 192	96 chords	—	0.00610	—	—
	455 × 170	12	—	0.00610	—	0.0
2	493 × 192	96	0.6655	0.00818	—	—
	455 × 170	12	0.6672	0.00805	0.3	−1.6
3	493 × 192	96	1.3111	0.01397	—	—
	469 × 178	24	1.3121	0.01376	0.08	−1.5
	455 × 170	12	1.3139	0.01349	0.2	−3.4
4	493 × 192	96	0.2569	0.00748	—	—
	455 × 170	12	0.2571	0.00747	0.06	−0.1
5	493 × 192	96	1.0039	0.03546	—	—
	455 × 170	12	1.0040	0.03542	0.01	−0.1
6	493 × 192	96	0.7990	0.01376	—	—
	455 × 171	12	0.7980	0.01359	−0.1	−1.2

reduced grid-resolution requirements.[12] Consequently, the conclusions which can be drawn from the present results apply strictly only to second-order centered difference schemes which use the scalar dissipation model described in Ref. 4 with the Baldwin-Lomax turbulence model. The results of the outer boundary-position studies also reflect the boundary-condition treatment used in ARC2D, including the far-field circulation correction. However, the results obtained provide useful guidelines for other flow solvers and turbulence models as well as a systematic approach for assessing their grid requirements.

Conclusions

A detailed investigation of the effects of grid clustering and refinement on the prediction of lift and drag in thin-layer Navier-Stokes computations of viscous airfoil flowfields has been presented. The effect of the location of the outer boundary of the grid has been examined as well. The flow cases studied exhibit a variety of flow features. The results can be summarized as follows. Grids W7A and A7A, which contain roughly 95,000 nodes, lead to spatial discretization errors of less than 1% in both lift and drag for most of the subsonic and transonic cases, respectively. Numerical errors of less than 1 % in lift only are obtained in all cases using grids N7A and N6A, which have roughly 48,000 nodes. Grid W7B, with roughly 24,000 nodes, produces less than 1% errors in lift for the subsonic cases. An outer boundary position of 12 chords introduces virtually no error in lift. Somewhat larger distances to the outer boundary are required to reduce the associated error in drag to below 1%. These results provide useful guidelines for determining the levels of grid refinement and the outer boundary position required to achieve a given level of accuracy for a range of flow conditions. The relatively grid-independent solutions obtained also provide an accurate assessment of the errors associated with the physical models used.

References

[1]Holst, T. L., "Viscous Transonic Airfoil Workshop Compendium of Results," AIAA Paper 87-1460, Honolulu, HI, June 1987.

[2]Zingg, D. W., "Viscous Airfoil Computations Using Richardson Extrapolation," AIAA Paper 91-1559, Honolulu, HI, June 1991.

[3]Zingg, D. W., "Grid Studies for Thin-Layer Navier-Stokes Computations of Airfoil Flowfields," AIAA Paper 92-0184, Reno, NV, Jan. 1992.

[4]Pulliam, T. H., "Efficient Solution Methods for the Navier-Stokes Equations," *Lecture Notes for the Von Karman Institute for Fluid Dynamics Lecture Series: Numerical Techniques for Viscous Flow Computation in Turbomachinery Bladings,* Von Karman Inst. for Fluid Dynamics, Brussels, Belgium, Jan. 20–24, 1986.

[5]Mehta, U., Chang, K. C., and Cebeci, T., "Relative Advantages of Thin-Layer Navier-Stokes and Interactive Boundary-Layer Procedures," NASA TM 86778, Nov. 1985.

[6]Gregory, N., and O'Reilly, C. L., "Low-Speed Aerodynamic Characteristics of NACA 0012 Airfoil Section, Including the Effects of Upper-Surface Roughness Simulating Hoar Frost," Aeronautical Research Council, Reports and Memoranda No. 3726, U.K., Jan. 1970.

[7]Harris, C. D., "Two-Dimensional Aerodynamic Characteristics of the NACA 0012 Airfoil in the Langley 8-Foot Transonic Pressure Tunnel," NASA TM 81927, April 1981.

[8]Cook, P. H., MacDonald, M. A., and Firmin, M. C. P., "Aerofoil RAE 2822—Pressure Distributions, and Boundary-Layer and Wake Measurements," AGARD-AR-138, May 1979.

[9]Maksymiuk, C. M., and Pulliam, T. H., "Viscous Transonic Airfoil Workshop Results Using ARC2D," AIAA Paper 87-0415, Reno, NV, Jan. 1987.

[10]Maksymiuk, C. M., Swanson, R. C., and Pulliam, T. H., "A Comparison of Two Central Difference Schemes for Solving the Navier-Stokes Equations," NASA TM-102815, July 1990.

[11]Barth, T. J., Pulliam, T. H., and Buning, P. G., "Navier-Stokes Computations for Exotic Airfoils," AIAA Paper 85-0109, Reno, NV, Jan. 1985.

[12]Swanson, R. C., and Turkel, E., "On Central-Difference and Upwind Schemes," Institute for Computer Applications in Science and Engineering, ICASE Rept. 90-44, Hampton, VA, June 1990.

Effect of Streamwise Pressure Gradient on the Supersonic Mixing Layer

Takashi Abe* and Katsushi Funabiki†
Institute of Space and Astronautical Science, Kanagawa 229, Japan
Hironobu Ariga‡
Musashi Institute of Technology, Tokyo 158, Japan
and
Katsumi Hiraoka§
Tokai University, Kanagawa 259-12, Japan

Introduction

THE mixing process in supersonic flow attracts much attention in scramjet engine research.[1] Extensive studies by not only experimental methods[2–4] but also by theoretical and numerical methods[5] have focused on this field. Among them, Papamoschou and Roshko[3] examined the compressibility effect on the mixing layer at the interface of the parallel supersonic flows and clarified the fact that the growth rate of the mixing layer is reduced by the compressibility effect in comparison with the one without the compressibility effect. In their study the mixing process was examined by means of the flow visualization technique by schlieren photography. Recently several researchers concentrated on enhancing the growth rate of the supersonic mixing layer,[4,5] since, e.g., the enhancement of mixing implies the improvement of the performance of the scramjet engine. In the present Note we attempt to clarify the effect of the streamwise pressure gradient of the flow on the growth rate of the mixing layer formed at the interface of the parallel supersonic flows. For this purpose the structure of the mixing layer was examined by the in-site measurement of the concentration ratio of the gas mixture.

Received July 16, 1991; revision received April 7, 1992; accepted for publication April 13, 1992.

*Associate Professor, Division of Space Transportation, Yoshinodai 3-1-1, Sagamihara. Member AIAA.

†Research Assistant, Division of Space Transportation.

‡Graduate Student, School of Engineering.

§Associate Professor, School of Engineering. Member AIAA.

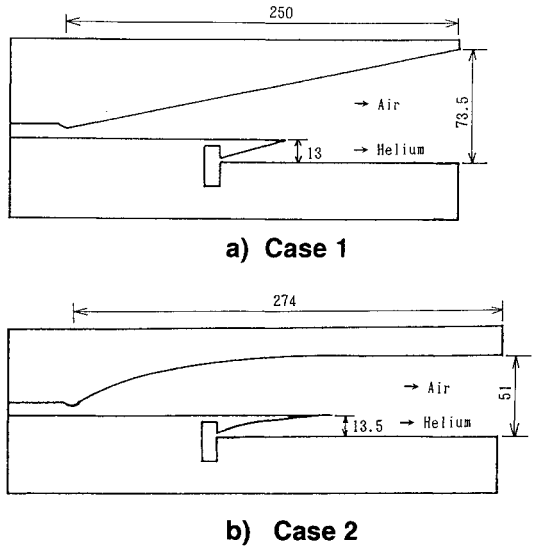

Fig. 1 Nozzle configurations: a) case 1; b) case 2.

Experimental Facility

To examine the effect of the streamwise pressure gradient on the mixing layer, we employed the wedge nozzle (case 1) to attain the supersonic flow having the streamwise pressure gradient and the shock-free nozzle (case 2) for comparison to attain the uniform supersonic flow. Two nozzles are combined to produce the parallel supersonic flows, as shown in Fig. 1. Both nozzles are two dimensional, and their transverse width is 100 mm. Separate two-dimensional supersonic flows are generated through each nozzle, and the mixing layer is generated at the interface of the supersonic flows. We note that in case 1 a slight nonuniformity along the vertical direction cannot be avoided as a result of the streamwise pressure gradient.

Supersonic flow is attained by supplying a high-pressure gas in a short time. For the lower nozzle, a pressurized helium gas with room temperature is employed, whereas for the upper nozzle, high enthalpy air is used which is produced at the stagnant region generated behind the reflected shock wave driven by the shock tube. That is, as far as the upper nozzle is concerned, the supersonic flow is generated by means of the shock tunnel. The reason for using the shock tunnel will be a future focus of the experiment. The shock tube is driven by using fast-action valves instead of the conventional rupture disks. These fast-action valves enable us to operate the facility in good reproducibility. The details of the experimental facility can be found in Ref. 6.

The nominal conditions for the airflow consist of the following: 2.93 kPa for static pressure, 226 K for temperature, 3.4 for the Mach number at the uniform region of the shock-free nozzle (or at the exit of the wedge-type nozzle), and 3.2×10^6 (1/m) for the Reynolds number. The nominal conditions for helium flow consist of the following: 2.93 kPa for static pressure, 43.4 K for temperature, 4.2 for the Mach number at the uniform region of the shock-free nozzle (or at the exit of the wedge type nozzle), and 1.74×10^7 (1/m) for the Reynolds number.

The steady flow is maintained during ~ 2 ms for the airflow while it is maintained sufficiently long for the helium flow to synchronize with the airflow. Synchronizing the timings of the generation of air and of helium flow, the steady parallel supersonic flows having a duration of 2 ms are obtained at the present facility.

Flow Visualization and In Situ Measurement by a Mass Sampling Probe

Schlieren photography of the flow generated for case 1 is shown in Fig. 2a. Papamoschou and Roshko[3] defined the visual growth rate of the mixing layer from the schlieren photography and examined the effect of compressibility on the visual growth rate of the mixing layer. However, it is rather difficult to discern the mixing layer from the photography. To avoid the ambiguity, the in situ measurement of the mixing process is attempted in the present experiment.

The basic idea for this measurement is to sample the mixture gas from the region inside the mixing layer and to analyze it by means of a mass spectrometer. From the measurement we can obtain a concentration ratio of helium at the region where the sampled gas is selected. The measurement system is composed of the probe mounted on the sampling valve driver which manages the gas sampling process, and the mass spectrometer. The gas entering the probe is steadily purged to avoid the effect of the gas entering the probe before the steady mixing layer is attained. When the probe is inserted into the mixing layer and the gas flow inside the probe becomes steady, the mixture gas inside the probe is sampled through the fast action valve equipped inside the probe and driven by the sampling valve driver. The tip of the probe is 1 mm ϕ in diameter. The sampled gas is introduced to the vessel that is attached to the mass spectrometer, and its component is analyzed by means of the mass spectrometer. The fast-action valve inside the probe is driven by an electromagnetic force supplied by a coil into which an electric current is discharged from a condenser bank and is driven correctly synchronizing with the steady mixing layer since the valve enables us to sample the gas in less than 1 ms.

The signal of the mass spectrometer for each species I_i is related to the flux of the species through the probe:

$$I_i \propto n_i v A$$

where n_i is the number density of the species, v the velocity, and A the area of the hole at the tip of the probe. The concentration ratio of the helium to the air is assumed to be equal to the ratio of helium to oxygen, which is one of the components of air. Hence, the ratio of the signal intensity of the mass spectrometer between helium and oxygen is related to the concentration ratio of the helium to the air:

$$n_{He}/n_{Air} = n_{He}/n_{O_2} = F(I_{He}/I_{O_2})$$

where the function F can determined by an appropriate calibration of the measurement system.

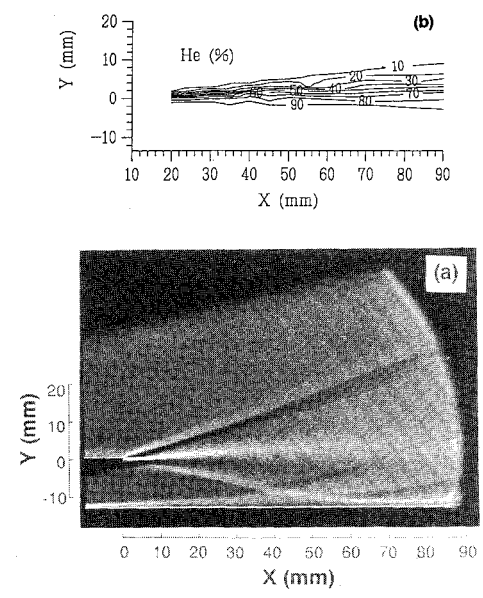

Fig. 2 Visualization for the flow of case 1: a) schlieren; b) contour of the helium concentration ratio.

Results

The distribution of the helium concentration ratio inside the mixing layer is measured by the present method. The measurements are conducted along a direction perpendicular to the flow (y direction) by 2-mm steps and along the flow direction (x direction) by 5-mm steps. Each set of measurement data is obtained by each operation of the facility. The error bar for the measurement at a fixed point for each operation is negligibly small. This accuracy was achieved by the good reproducibility of the flow, which is a very important feature of the present facility. The concentration ratio contour (Fig. 2b) allows the growth of the mixing layer to be seen clearly. As can be seen for Fig. 2b, the mixing layer grows along the flow direction. Needless to say, the location of the mixing layer that can be discerned from the schlieren photography of the flow is almost the same as the one represented by the concentration ratio contour.

We define the width of the mixing layer b as the length from the location of 10% to that of 90% in the concentration ratio of helium. The mixing layer width increases almost monotonously with the flow direction. Hence, we define the growth rate db/dx of the mixing layer by applying the linear curve-fitting method to the plot of the measured mixing layer width vs the stream direction. The normalized growth rates for cases 1 and 2 are 0.13 and 0.07, respectively. That is, the growth rate in case 1 is about two times larger than the one in case 2. The normalization was conducted by the growth rate without the compressibility effect.[3] For comparison the visual growth rates for cases 1 and 2 are 0.11 and 0.06, respectively. The visual growth rate was obtained from the schlieren photography of the flows.[3] The visual growth rates almost agree with the ones obtained from the measurement of the concentration ratio.

The effect of flow compressibility on the visual growth rate is shown in Fig. 3, which is the reproduction of the results of Papamoschou and Roshko.[3] In the figure the normalized visual growth rate is plotted against the compressibility parameter M^+ (Ref. 7). The present result for the growth rate is plotted by open triangles for case 1 and filled triangles for case 2, respectively. As expected, the present results for the shock-free nozzle almost agrees with those of Papamoschou and Roshko.[3] The slight difference between them can be attributed to the ambiguity or the measurement of the visual growth rate. Since the growth rate in case 2 can be considered to be the same as the existing value, we can conclude that the effect of the streamwise pressure gradient enhances the growth rate of the mixing layer without the effect.

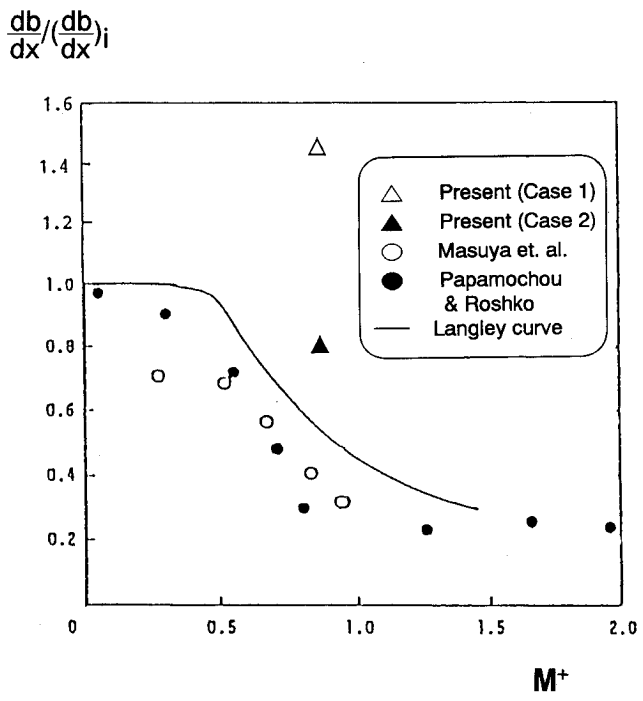

Fig. 3 Normalized growth rate of the mixing layer vs the compressibility factor M^+. The $(db/dx)_i$ is the growth rate without the compressibility effect.

Discussion

The present result shows that the growth rate of the mixing layer is affected by the streamwise pressure gradient, and the growth rate is enhanced in the wedge-type nozzle in comparison with the one in the shock-free nozzle. The enhancement of the growth rate may be correlated to the vortex generation, which is implied by the baroclinic torque appearing in the equation for the vorticity ω:

$$\frac{D\omega_z}{Dt} = -\omega_z\left(\frac{\partial U_x}{\partial x}+\frac{\partial U_y}{\partial y}\right)+\frac{1}{\rho^2}\left(\frac{\partial P}{\partial x}\frac{\partial \rho}{\partial y}-\frac{\partial \rho}{\partial x}\frac{\partial P}{\partial y}\right)$$

where $D\omega_z/Dt$ is a rate of change of vorticity following a fluid element, U is the flow velocity, the first term on the right-hand side is related to the fluid expansion (or compression), and the second term is the baroclinic torque. In the present system of parallel supersonic flows, the significant density gradient exists at the interface since the density at the air and heliun flow is about 4.5×10^{-2} and 3.1×10^{-2} kg/m^3, respectively. Also, in the wedge-type nozzle (case 1), there is a pressure gradient along the flow that is inherent to Mach number changes from 3.4 at the start of the mixing layer to 3.9 at the exit of the nozzle. These gradients normal to each other produce the baroclinic torque of 2.6×10^7 s^{-2}, while the typical vorticity of the mixing layer is 1.1×10^5 s^{-1}. Since the vorticity accelerates the mixing, the vorticity produced by the baroclinic torque is a candidate for the cause of the enhancement of the growth rate of the mixing layer.

Conclusions

We have conducted the in situ measurement of the concentration ratio inside the mixing layer to examine the streamwise pressure gradient effect on the mixing layer at the interface between the parallel supersonic flows. When a streamwise pressure gradient exists, the growth rate of the mixing layer is enhanced in comparison to the one without the gradient. As for the cause of the enhancement, the baroclinic torque produced by the streamwise pressure gradient is a candidate for the cause of the enhancement.

Acknowledgment

The authors are grateful for the assistance of T. Kohama throughout this study.

References

[1]Ferri, A., "Mixing Controlled Supersonic Combustion," *Annual Review of Fluid Mechanics,* Vol. 5, 1973, pp. 301–338.

[2]Chinzei, N., Masuya, G., Komuro, T., Murakami, A., and Kudo, K., "Spreading of Two-Stream Supersonic Turbulent Mixing Layers," *Physics of Fluids,* Vol. 29, No. 5, 1986, pp. 1345–1347.

[3]Papamoschou, D., and Roshko, A., "Observations of Supersonic Free Shear Layers," AIAA Paper 86-0162, Jan. 1986.

[4]Menon, S., "Shock-Wave-Induced Mixing Enhancement in Scramjet Combustors," AIAA Paper 89-0104, Jan. 1989.

[5]Kumar, A., Bushnell, D. M., and Husani, M. Y., "A Mixing Augmentation Technique for Hypervelocity Scramjets," AIAA Paper 87-1882, June 1987.

[6]Hatakeyama, M., Funabiki, K., and Abe, T., "An Experimental Study of Supersonic Mixing Process by Using Shock Tunnel Using Quick-Action Valves and Quick-Mass-Sampling Probe Technique," *Journal of the Japan Society for Aeronautical and Space Sciences,* No. 425, 1989, pp. 278–284 (in Japanese).

[7]Bogdanoff, D. W., "Compressibility Effects in Turbulent Shear Layers," *AIAA Journal,* Vol. 21, No. 6, 1983, pp. 926, 927.